New York Science Journal

Websites:
http://www.sciencepub.net/newyork
http://www.sciencepub.net

Emails:
newyorksci@gmail.com
editor@sciencepub.net

MARSLAND PRESS
Multidisciplinary Academic Journal Publisher

Comparative Analysis on the Seismic Performance of Precast Segmental and Hybrid Bridge Columns

Jahangir Badar

Department of Civil Engineering, Nanjing University of Science and Technology, Xiaolingwei Street 200, Nanjing 210094, P. R. China
Jahangirbaloch@njust.edu.cn

Abstract: This paper studies the cyclic performance of segmental columns with different construction details and varying types of post-tensioned tendons by using three-dimensional finite element (FE) commercial software ABAQUS. The modeling techniques showed excellent calibration with an overall error of less than 10%. The influence of axial loads, the orientation of post-tensioned tendons, and their combined influence are analyzed to improve the lateral strength and energy dissipation capacities of segmental columns. Detailed parameter analysis concluded that the lateral strength and energy dissipation capabilities could be significantly improved by utilizing cast-in-place (CIP) bottom segments instead of segmental. The energy dissipation capacities of hybrid bridge columns (HBCs) are far superior to precast segmental bridge columns (PSBCs), but with much larger residual displacements. The orientation of post-tensioned (PT) tendons at the middle while restricting the axial load ratios to 0.15 highlighted efficient seismic performance. Finally, for HBCs, the PT tendons should be located in the middle and edges of the specimen to control excessive damage and significant drops in the lateral strength and energy dissipation capacities.

[Jahangir Badar. **Comparative Analysis on the Seismic Performance of Precast Segmental and Hybrid Bridge Columns.** *N Y Sci J* 2020;13(6):39-56]. ISSN 1554-0200 (print); ISSN 2375-723X (online). http://www.sciencepub.net/newyork. 6. doi:10.7537/marsnys130620.06.

Keywords: Precast segmental bridge columns; Cyclic performance; Numerical analysis; Hybrid bonded tendons; Axial loads; Post-tensioned tendons.

1. Introduction

Prefabricated bridge design has lately attained a growing consideration in the bridge engineering community due to its several advantages, including accelerated production speed, limited environmental repercussions, higher production quality, improved site protection, and reduced endurance cost [1-4]. The challenges of aging bridges, which need retrofitting, stabilization, rehabilitation, and replacement, are increasing worldwide. In the face of these increasing challenges, there is a strong drive to develop technologies to facilitate bridge construction. Different transportation agencies adopt the mantra "get in, get out, stay out," which means constructing the structures quickly and efficiently without compromising on the quality aspects of it [4-8].

The precast segmental bridge columns (PSBCs) are directly related to the seismic performance of the whole bridge system. During a seismic event, the segmental columns produce a small residual displacement due to the excellent recentering capabilities provided by the post-tensioned tendons but, the damage is not restricted due to the deficient energy dissipation capacities provided by these systems [9-11]. Various techniques are proposed to enhance the cyclic performance of prefabricated segmental bridge columns [12-24]. An efficient technique has been the usage of yielding components in the plastic hinge region or bottom sections of the prefabricated piers such as mild steel bars crossing the segmental joints commonly referred to as energy dissipation (ED) bars [12-14], exterior dissipators [15-16], shape memory alloy (SMA) bars [17-18], hybrid steel bars [19], elastomeric pads [20], and FRP steel jackets [21-22]. Some scholars also proposed the introduction of new high-performance materials, such as fiber reinforced composites, cement- based composites, fiber-reinforced concrete, and ultra-high performance concrete [23-24]. Overall, these methods can enhance the energy dissipation capacity and ductility of prefabricated segmental piers; however, the relativity high cost and complicated designs have limited their practical applications.

Researchers have recently proposed a mix of cast-in-place (CIP) and precast segments to improve the system's energy dissipation. This innovative system was proposed by Ou. *et. al* [25] for the first time, which utilized an innovative prefabricated segmental bridge pier using cast-in-place (CIP) construction for the lower parts and segmental

construction for the upper regions. The combination of rocking mechanism with rigid rotations for the upper segments and formation of plastic hinges in the bottom segment leads to improved hysteric energy, energy dissipation, and adequate displacement capacity, ductility, and residual plastic deformations. Kim. *et. al* [26] tested and analyzed a new prefabricated segmental column based on the concept proposed by Ou. *et. al* [25]. The length of the CIP region was defined for the segmental column designed by Kim. *et. al* [26] by measuring the latent plastic hinge height. The findings illustrated proficient ductility and energy dissipation capability although no post-tensioned tendons were used in their analysis. However, the quantitative influence of the different design parameters on the structural capacity of hybrid bridge columns (HBCs) has rarely been analyzed. Therefore, further comparative studies are required to determine the exact advantages of the emulative hybrid pier system to the commonly employed PSBCs.

In this study, a simpler HBC design is proposed. The method employs CIP construction for the potential plastic hinge region (inherent plastic hinge region is designated as the greater of column diameter and 1/6th the extent from column base to the loading point) and precast segmental blocks for the upper segments. A similar experimental PSBC model based on the studies of Zhang. *et. Al* [27] is selected with every segment consisting of prefabricated components for comparative analysis. The HBCs and PSBCs are designed by utilizing finite-element modeling (FEM) platform *ABAQUS*. The numerical model is validated against the experimental studies in order to perform detailed parametric analysis. The parameters of interest include the influence of axial load ratios, post-tensioned tendon area, the combined influence of changing axial load and orientations of post-tensioned tendons, and finally, the impact of innovative hybrid bonded tendons in PSBCs and HBCs respectively. The essence of the study is to highlight the structural advantages of HBCs to PSBCs in terms of lateral strength, energy dissipation, and residual deformations. The impact of seismic performance indicators such as bearing capacity, energy dissipation, and residual deformations is expected to provide engineering design reference for PSBCs and HBCs.

2. Key Design Methodologies

2.1 Structural Performance of PSBCs and HBCs under cyclic loading

The PSBC is built by piling the segments upside down. The post-tensioned tendons are usually the only reinforcement continuous across the segment joints, which provide the clamping force, and the mild steel bars are discontinuous across the joints [28]. As the longitudinal reinforcements are discontinuous at the joints, the piers exhibit little plastic deformation because the segment joints attract most of the tensile deformation. The plastic deformations of precast segmental bridge columns (PSBCs) are typically small under earthquakes, which enables strong re-setting abilities. However, due to substantial joint openings, primarily when the PSBCs are employed in medium-high seismic regions can lead to severe cracking and crushing at the joints, along with making the performance of segmental joints uncertain. Additionally, the hysteric energy dissipation of PSBCs is very low, particularly compared to monolithic bridge columns (MBCs) with an equivalent viscous damping ratio of 4~5%.

The current seismic design codes are based on MBCs; therefore, their application on PSBCs is invalid due to the difference in seismic behavior. Hence, the PSBCs are designed with an elastic design approach that restricts the plastic deformations [25]. Due to these limitations, the PSBCs in strong seismic regions require large cross-sections size and an additional amount of post-tensioned tendons, which invariably increases the amount of material and cost.

Taking the previous research of OU. *et. al* [25] and Kim. *et. al* [26] as motivation, this article presents a new design to increase the lateral strength and energy dissipation of prefabricated columns. The proposed HBC consists of the standard orientation of post-tensioned tendons and simpler cross-section as opposed to preceding studies. The upper segments of the proposed HBC are composed of segmental blocks, while the bottom segment is cast monolithically with the foundation. The longitudinal and transverse reinforcements pass through the bottom joint and penetrate the foundation. Combining the formation of a plastic hinge mechanism at the CIP portions and non-linear behavior of segmental joints for the upper segments will likely increase the energy dissipation and ultimate strength of HBCs. The post-tensioned tendons will likely enhance the recentering abilities of HBCs as compared to conventional CIP piers, thereby reducing the plastic deformations and restricting the residual drifts under manageable levels.

2.2 Design of Hybrid Post-Tensioned Tendons

Hybrid post-tensioned is a novel design that aims to take advantage of both unbonded and bonded properties of post-tensioned tendons. Unbonded post-tensioned tendons provide the excellent recentering capability to the segmental piers, whereas limited lateral strength and energy dissipation are its counterproductive behavior [29]. In contrast, bonded tendons can increase the lateral strength and, most importantly, energy dissipation capacities of the system. However, the usage may lead to the yielding of tendons, which can endanger the performance of

piers due to reduced shear resistance and strength degradation [30-31]. Therefore, hybrid bonding technique utilizes the hybrid bonding in every post-tensioned tendon individually in the carefully selected regions to enhance the lateral strength and energy dissipation capacities of segmental columns. The idea is to create a strong bond between the steel grout and tendons by injecting cementitious materials into the grout along a certain length of the column and keeping the rest of the tendon unbonded. The hybrid bonded post-tensioned tendons will likely lead to greater lateral strength due to the development of strong bonds, and enhanced energy dissipation will be obtained by induced cracks and damage to the concrete around the strands. While keeping the tendons unbonded in other regions will lead to retention of the self-centering capabilities.

One of the objectives of this research is to design a novel hybrid bonded tendons by systematically studying the seismic performance of these new tendon systems in PSBCs and HBCs. The goal is to obtain optimum performing prefabricated segmental bridge columns with improved lateral strength, energy dissipation while keeping residual drifts to manageable levels so that after the earthquake, they can easily be repaired or retrofitted respectively. The successful design of PSBCs and HBCs with hybrid bonded post-tensioned tendons will lead to boost the confidence of designers and engineers to increase the usage of segmental columns in medium-high seismic regions.

3. Modeling Description

3.1 Specimen Design and Modeling approach

At present, a three dimensional (3D) finite element (FE) method [32], and fiber model analysis method [33] is mainly used for non-linear numerical analysis of prefabricated assembled piers. Although the latter model has strong convergence ability and fast calculation speed, the former model's analysis is more intuitive than the fiber analysis method, and the calculation results are far more accurate, especially when contact analysis problems are considered. Therefore, this paper uses the finite element method to analyze the proposed columns based on ABAQUS/Standard platform.

Three dimensional finite-element (FE) models are generated based on the experiments performed by Zhang. *et. al* [27]. The prefabricated bridge column denoted as PSBC-1 with a scale factor of 1/4th is modeled and used in this study. The experimental model was designed with the 1/4th scale of original columns used in the practical applications due to the limitation of facilities. It was observed in the experiment that the 1/4th model could accurately predict the seismic performance, and the difference between the full scale and 1/4th scale model is limited. Hence, for the accuracy of numerical results, 1/4th scale model is utilized. The material properties are shown in **Table 1**, whereas **Fig. 1** highlights the cross-sectional and reinforcement details of PSBC-1.

The components made of concrete are modeled by using eight-node 3D brick elements (C3D8R). The concrete damage plasticity (CDP) model is utilized to simulate the behavior of reinforced concrete columns subjected to dynamic loadings [34]. The stress-strain relationship of concrete developed by Mander. *et. al* [35], and further enhanced by Lubliner. *et. al* [36], Lee. *et. al* [37] is used in this study. Truss element (T3D2) is used to simulate the steel bars and spiral reinforcements in precast segments. Embedded regions are defined with the steel cage as an embedded region and the whole model as a host region to simulate core concrete confinement, as shown in **Fig. 2** [34].

Table 1 Material properties of prototype model

Component	Property	Value
Concrete	Strength (MPA)	47.0
	Poisson's ratio	0.2
	Elastic modulus (GPA)	34.5
Transverse reinforcements	Yield stress (MPA)	335.0
	Poisson's ratio	0.3
	Elastic modulus (GPA)	210
Longitudinal reinforcements	Yield stress (MPA)	335.0
	Poisson's ratio	0.3
	Elastic Modulus (GPA)	200
Prestressed Tendons	Yield stress (MPA)	1670
	Ultimate Stress (MPA)	1860
	Poisson's ratio	0.3
	Elastic Modulus (GPA)	195

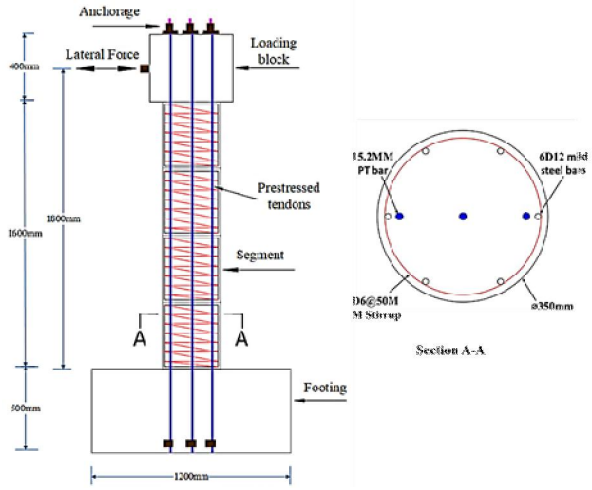

Fig. 1 Cross-sectional and reinforcement details of prototype model

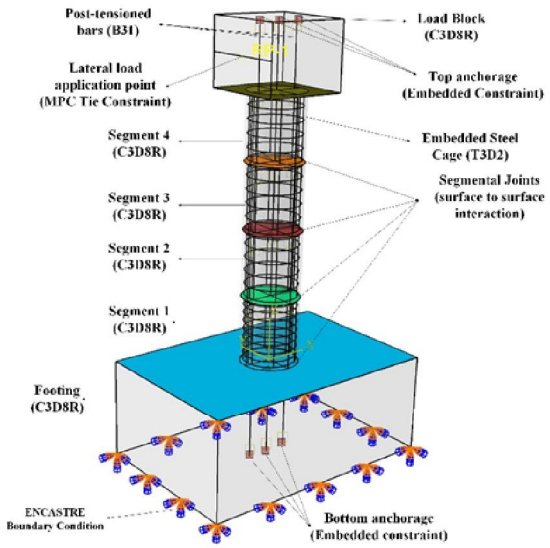

Fig. 2 Model details of prototype model

Prestressing tendons are simulated by beam elements (B31), both ends are cut a certain distance and are embedded into loading block and bearing platform to establish anchorage. Beam elements (B31) are used to model components whose one direction (length in this case) is considerably more significant than the other two, together with a dominant stress profile along the component's length. The provision of a rotational degree is another significant explanation for designing post-tensioned tendons with beam elements (B31). The unconstrained part of post-tensioned tendons is prestressed by a falling temperature method through a predefined material expansion coefficient of 1.0×10^{-5}. The initial prestressing levels of 25% (PT L & R) and 30% (PT-MID) are selected to preserve the axial force and reentering abilities of the column [28, 38]. The elastic-perfectly plastic model was used to simulate the stress-strain aspect of the steel reinforcements and prestressed tendons [39].

ENCASTRE boundary condition is used to simulate the fixed boundary condition. The joint opening/closing mechanism under cyclic loadings was defined by surface to surface contact elements. The surface with higher rigidity is selected as the master surface, and another surface is selected as a slave. The normal behavior between the contact pairs is defined as hard contact to ensure joint opening and closing. The tangential behavior is defined as "penalty," and the friction factor is selected as 0.5 [11]. The loading is applied in two stages. The first stage involves the application of axial loads through prestressed tendons. In the second stage, lateral displacement controlled cyclic loadings were imposed on the reference point of loading block with pre-defined drift values. The loading protocols are shown in Fig. 3 respectively.

The same prototype model is utilized to model a hybrid bridge column (HBC), with the only difference being that of the bottom segment. The longitudinal and transverse reinforcements pass through the bottom joint and penetrate into the foundation. As the bottom segment is cast monolithically with the foundation, the bottom joint will not exhibit a rocking mechanism, and hence is tied with footing [40-41]. The rigid body constraint is utilized with footing as a rigid body, bottom segment nodes as tie nodes, and reference point controlling the overall motion, as shown in **Fig. 4**.

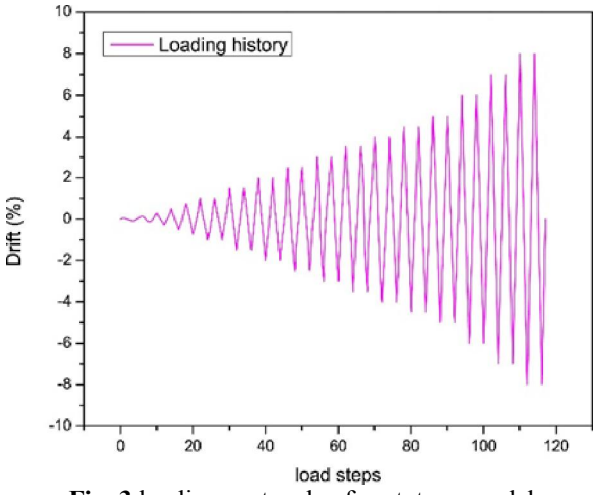

Fig. 3 loading protocols of prototype model

3.2 Model Validation

In this research, the numerical models are calibrated against the experimental results in terms of force-displacement hysteric curves and damage modes at the ultimate drift level as shown in **Table 2**, and **Fig.**

5, and **Fig. 6** respectively. In terms of force-displacement hysteric curves, excellent calibration was observed with an overall error of less than 10%. **Figure 6** presents the damage modes of the test specimen and the numerical model. It is highlighted in **Fig. 6(a)** that the concrete cover on one side of the bottom section spalled at the ultimate drift level of the test due to the accumulation of large axial compressive stresses. The numerical model, as seen in **Fig. 6(b)** simulated concrete damage. The black portion shows the concrete elements having higher axial strains that top the ultimate strain of the unconfined concrete respectively.

The slight differences in numerical and experimental results can be attributed to the fact that the lateral forces obtained in the numerical simulations are almost symmetric. In contrast, they are slightly asymmetric in the experiments due to installation errors and unsymmetrical damage of the test specimens. The other causes include errors in predicting concrete damage. Further models should be simulated to know the exact cause of errors in the prediction of concrete damage. The application of the CDP model for concrete inelastic behavior and surface-to-surface contact for joint activity can predict the residual deformations of the PSBCs specimens under cyclic loading satisfactorily. Overall, the results demonstrate that the numerical models can accurately predict the hysteric behavior of column specimens under the action of cyclic loads.

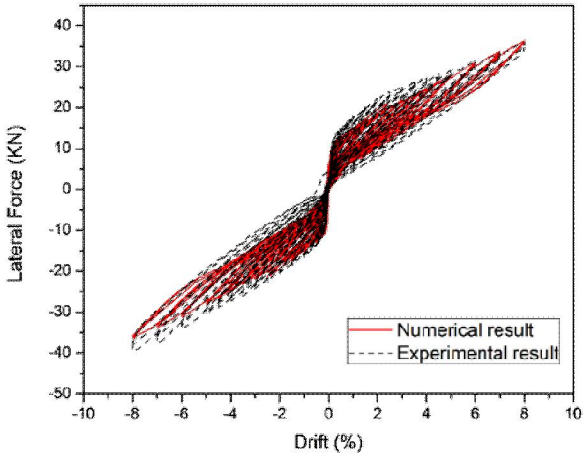

Fig. 5 lateral strength of numerical and experimental model

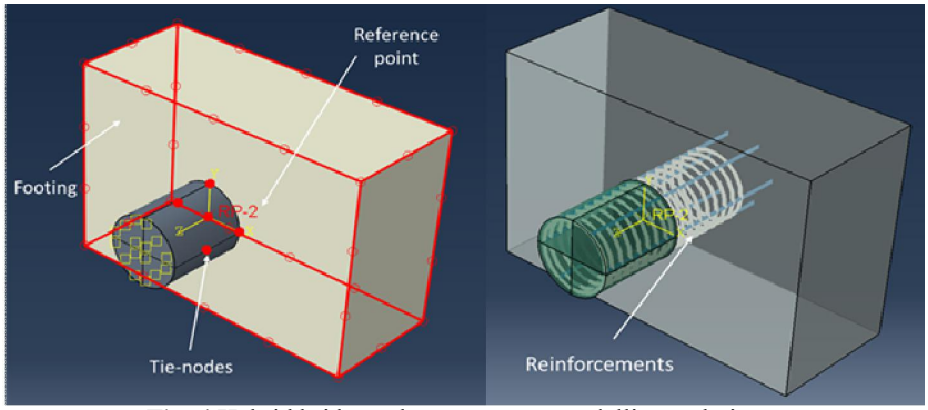

Fig. 4 Hybrid bridge column segment modelling technique

Table 2 Model calibration results

Drift ratio (%)	Experiment (Kn)	Numerical (Kn)	Error (%)
1	17.69	16.01	9.49
-1	-15.94	-14.94	6.27
3	23.96	21.61	9.8
-3	-22.96	-21.23	7.53
5	28.12	27.65	1.67
-5	-29.26	-27.6	5.67
7	32.16	33.36	6.32
-7	-35.02	-33.28	4.96
8	35.93	35.91	0.05
-8	38.53	-35.83	7

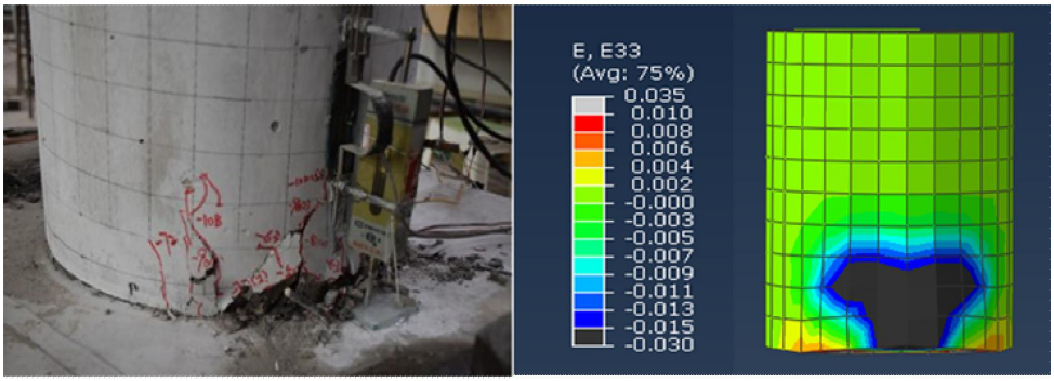

Fig. 6 Damage modes of experimental and numerical model

4. Results and Discussion

4.1 Influence of Axial Load Ratios

The axial loads play a vital role in the cyclic performance of columns. In the case of the precast column, it is the gravity load (deck weight and column self-weight) and the prestressing force, which provide moment resistance against overturning [42-43]. In this research the axial loads are calculated by the following formula;

$$\text{Axial load} = \frac{N}{f'c\, A_g}$$

Where, N= Initial prestressing force; f'c= Compressive strength of concrete; Ag=gross sectional area of concrete

The increase in the axial load ratios by increasing the initial prestressing force leads to the higher ultimate strength and small residual drift [44]. On the other hand, increasing the axial loads will lead to higher compressive stresses when the column segments rock back and forth with respect to each other [45, 46]. Higher axial compressive stresses can result in concrete crushing failure of the column and reduce the column's ductility. Therefore, in this section, axial loads are increased by increasing the post-tensioned area while maintaining the initial prestressing levels at 25% and 30% of (f'cAg). The model details are described in **Table 3.**

At axial load 0.1, the hybrid bridge column (HBC) can demonstrate higher lateral strength than the precast segmental bridge column (PSBC), highlighting the advantages of using a hybrid system. Both the systems showed excellent re-centering abilities with the residual plastic displacement of less than 1%. The residual plastic deformation for PSBC is minimal (0.39mm in the positive direction), whereas the HBC specimens have more significant plastic deformation (6.59mm in the positive direction). The difference in the plastic deformations of HBCs and PSBCs can be attributed to the development and plastic hinges in the bottom segment of HBC, cast monolithically with the foundation, as shown in **Fig. 7**. The more prominent cosmetic damage in the form of concrete spalling and higher strains generated by the strain penetration in the foundation due to the transverse and longitudinal reinforcements crossing the bottom joints leads to increased residual deformation. HBC-A1 can generate a lateral strength of 41.1KN, which is 15% greater than PSBC-A1 at the ultimate drift, as shown in **Fig. 8**. The PSBCs lack in dissipating sufficient energy, whereas HBC can overcome this particular issue. Cumulative energy dissipation of HBC-A1 was recorded as 1096 KN-mm, which is 66% greater than PSBC-A1, as visible in **Fig. 8**. Hence, the advantages of hybrid systems are far greater in terms of energy dissipation at an axial load of 0.1 for a type of column studied in this research.

Table 3. Specimen details of PSBCs and HBCs

Specimen	Bonding Condition	Post-tensioned tendon Area	Axial load ratio
PSBC-A1	Unbonded	3D15.2mm	0.1
PSBC-A2	Unbonded	3D17.8mm	0.15
PSBC-A3	Unbonded	3D21.6mm	2
HBC-A1	Unbonded	3D15.2mm	0.1
HBC-A2	Unbonded	3D17.8mm	0.15
HBC-A3	Unbonded	3D21.6mm	2

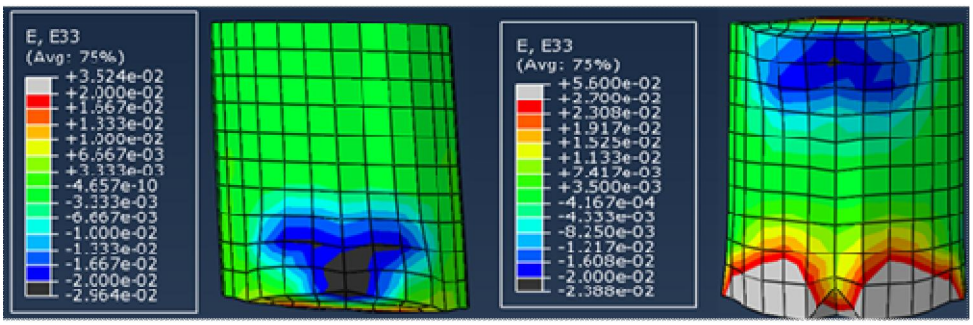

a) PSBC **b) HBC**

Fig. 7 Maximum Compressive strains of bottom segments a) PSBC b) HBC

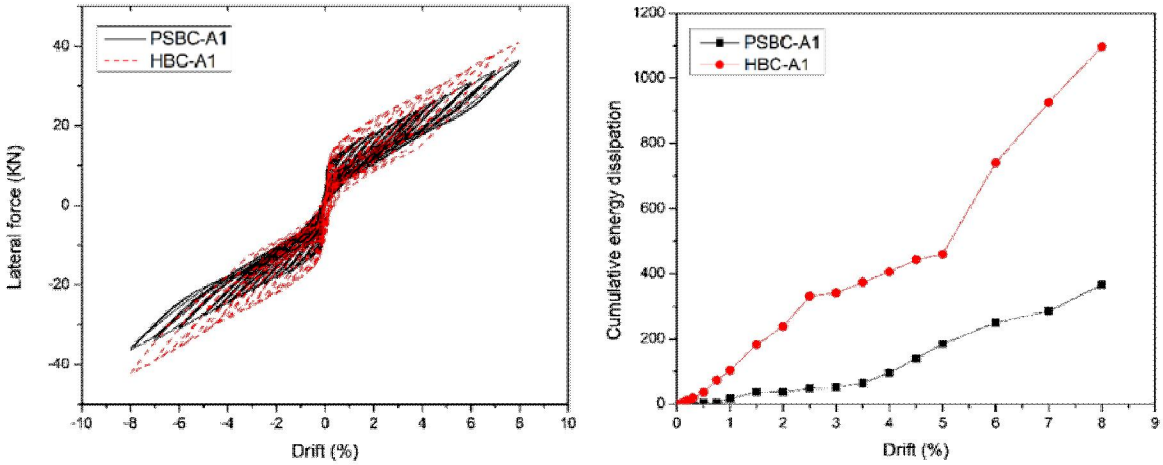

Fig. 8 Hysteric and energy dissipation curves of HBC and PSBC

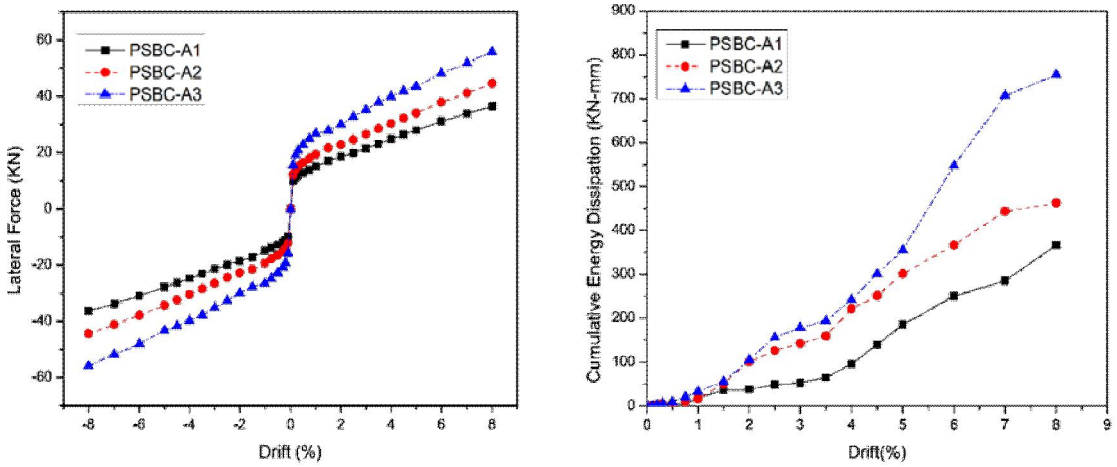

Fig. 9 Backbone and energy dissipation curves of PSBCs with increasing axial load ratios

4.2 Influence of axial load ratios in PSBCs

Precast segmental bridge columns with axial load ratio of 0.1, 0.15, and 0.2 are studied. The backbone curves are shown in **Fig. 9**, which are generated by taking average load between both positive and negative cycles and plotting them against each drift level. Cumulative energy dissipation curves that describe the area enclosed by each load cycle are also shown in **Fig. 9**. The ultimate strength of the column increases with the increasing axial load ratios. Also, for the selected axial loads, the column stiffness after yielding remained positive as implied by no evidence of strength degradation for the designed PSBCs. The displacement capacities and ductility for

columns will also not decrease drastically by keeping the axial loads to 0.2. All the columns analyzed showed excellent recentering abilities. The energy dissipation gradually increased with peak energy dissipation observed by PSBC-A3, which is 52% greater than PSBC-A1. Hence, it is proved that designing the PSBCs by keeping the axial load ratio to 0.2 can lead to better cyclic performance than PSBCs with very low or high axial load ratios, respectively.

4.3 Influence of axial load ratios in HBCs

The HBCs at an axial load ratio of 0.1 exhibited better cyclic performance than its PSBC counterpart. Increasing the axial loads of HBCs can lead to an improvement in the characteristics which govern the cyclic performance. As the axial loads were carefully selected, the specimens showed improvement in the lateral strength with the increase in the axial loads. Likewise, the PSBCs, HBCs stiffness after yielding remained positive with no signs of strength degradation. The HBCs were able to limit the plastic deformation under safety limits. There was a substantial increase in the energy dissipation of HBCs with peak-dissipated energy recorded of 2678 KN-mm at 0.2 axial load ratio, which is 60% greater than HBC-A1, shown in **Fig. 10**. Proper design of axial loads can lead to an improvement in the cyclic performance of HBCs, especially the energy dissipation capacities, which validates the motivation for designing such a system, respectively.

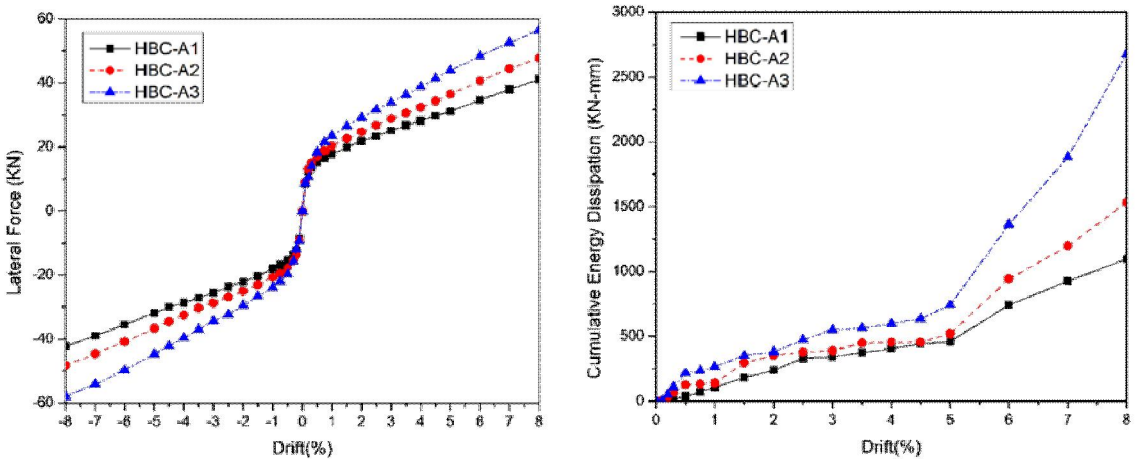

Fig. 10 Backbone and energy dissipation curves of HBCs with increasing axial load ratios

4.4 Comparative analysis of HBCs and PSBCs with different axial load ratios

The comparative analysis between HBCs and PSBCs will lead to understanding the influence of axial load ratios. **Table 4** shows the lateral strength, energy dissipation, and residual plastic displacement of specimens. As discussed in the previous sections, it is evident that increasing the axial load increases the lateral strength and energy dissipation of the specimens designed. The residual plastic displacement remained negligible by increasing the axial load ratios for PSBCs; on the other hand, HBCs showed a minimal increase for axial load ratio of 0.15 and a gradual increase in the plastic deformation for an axial load of ratio 0.2. The difference in the lateral strength for HBCs and PSBCs reduced with the increase in the axial load ratio.

For example, HBC with an axial load ratio of 0.1 was able to generate a 15% greater lateral strength whereas, only a 3.52% increase was observed for an axial load ratio of 0.2. However, the energy dissipation capacities continued to increase with an increment in the axial load ratios. HBCs dissipated 66.31% and 71.84% greater energy than the PSBCs specimens with axial loads of 0.1 and 0.2. The lack of energy dissipation in PSBCs can be attributed to the lower level of damage to the bottom segments, which results in minimal residual deformations.

Table 4. Response parameters of PSBCs and HBCs

Specimen	Lateral Strength (Kn)	Residual displacement (mm)	Energy dissipation (Kn-mm)	Axial load ratio
PSBC-A1	35.91,-35.83	0.39,0.78	366.32	0.1
PSBC-A2	44.62, -44.55	0.5, 1.02	461.86	0.15
PSBC-A3	54.54, -54.63	0.59, 1.24	754.55	2
HBC-A1	41.11, -42.25	6.59, -3.83	1096.35	0.1
HBC-A2	47.7, -48.2	6.95,-4.16	1532.717	0.15
HBC-A3	56.53, -57.94	11.45,-8.813	2678.112	2

4.5 Orientation of Post-Tensioned Tendons in Segmental Columns

The Post-tensioned tendons play an essential role in the cyclic performance of columns [47-49]. As the PSBC displaces laterally under earthquake excitation, a wide flexural crack is formed at the interface between the column base and foundation as the column rotates rigidly about its compression toe. In contrast, for the cast-in-place section, plastic hinges are formed, which results in the appearance of the flexural cracks and yielding of reinforcements, resulting in tensile cracking. The prestressing steel is stretched once the base crack opening extends to the location of the tendon. If the tendons are not entirely bonded over the height of the column, incremental strains will not concentrate at a crack; instead, strains will be distributed along the whole length of the tendon. This phenomenon is vital for several reasons. First, the facility to convey shear across the segment interfaces by shear friction is reliant on the clamping force produced by the prestressing tendon. The column stiffness is also reliant on the prestressing force. Finally, the restoring force provided by the column by the prestress is maintained during and after the earthquake.

Given this hindsight, post-tensioned tendons positioning can influence the cyclic performance of both the PSBCs and HBCs. Hence, the tendons are oriented at the center, center and edge, and only edges of the column. The orientation of Post-tensioned tendons is shown in **Fig. 11**, and the specimens detail are mentioned in **Table 5**.

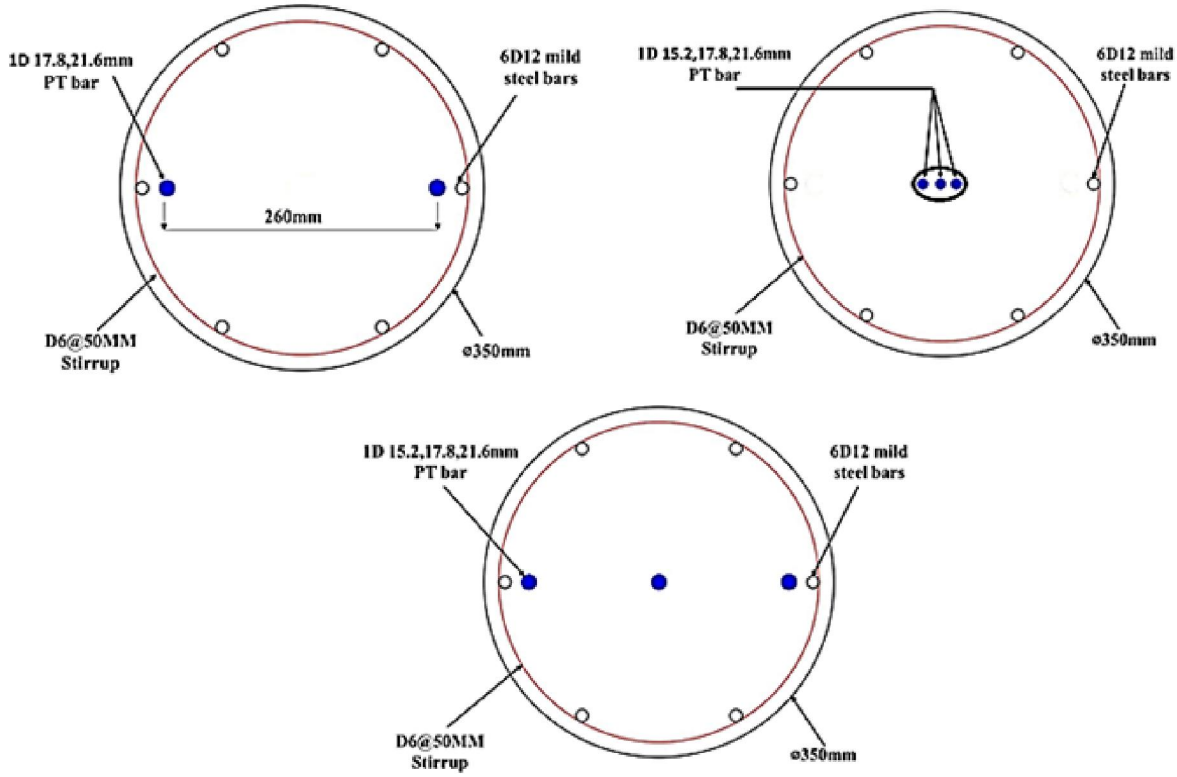

Fig. 11 Orientations of post-tensioned tendons in piers

Table 5. Specimen details for PSBCs and HBCs with different post-tensioned orientations.

Specimen	Bonding Condition	Post-tensioned tendon area	Orientation	Axial load ratio
PSBC-A11	unbonded	3D15.2mm	Middle and edge	0.1
PSBC-A21	unbonded	3D15.2mm	Middle	0.1
PSBC-A31	unbonded	2D17.8mm	Edge	0.1
HBC-A11	unbonded	3D15.2mm	Middle and edge	0.1
HBC-A21	unbonded	3D15.2mm	Middle	0.1
HBC-A31	unbonded	2D17.8mm	Edge	0.1

For PSBCs, the tendons placed at the center and edge show excellent recentering abilities and a steady improvement in the lateral strength. The energy dissipation remained on the lower side due to the narrow cyclic shape, as shown in **Fig. 12(a).** The tendons placed only at the edges also showed similar characteristics with a slight improvement in the lateral strength. The PSBC with tendons oriented at the edges showed a slight decrease in the energy dissipation capacities due to the slightly more plump shape. The major difference occurred when the axial load ratio was maintained at 0.1, and the tendons were placed at the geometric centroid. Wide cyclic loading curves were obtained at each drift, which substantially improved the energy dissipation of such piers, as shown in **Fig. 12(b)**. The difference in the accumulation of lateral resistance is quite evident in **Fig. 12(c)**.

For PSBCs with tendons oriented in the center, the majority of lateral resistance occurs at the initial stages. The non-availability of tendons at the edges results in substantial damage to the edges of the specimen, resulting in higher lateral resistance than PSBCs having tendons at the edges. After 0.75% drift softening of the lateral resistance curve happens, this softening pattern continues until a 3% drift followed by a gradual increase in the lateral resistance. The increase in the tendon stress occurs after a significant drift of the pier takes place since the post-tensioned tendon is placed at the geometric centroid of the pier. Additionally, the stretching of PT tendons is less than that of tendons placed at the edges, which decreases the amount of stress transformed, hence reducing its influence in contributing significantly to the improvement of lateral strength, respectively. This fact, along with increased material non-linearity caused by extensive damage to compression toe of the PSBCs with tendons oriented at the center, leads to the softening of the cyclic curves. To validate these fact specimens with increased axial load ratios will be discussed to analyze the vulnerability of such specimens.

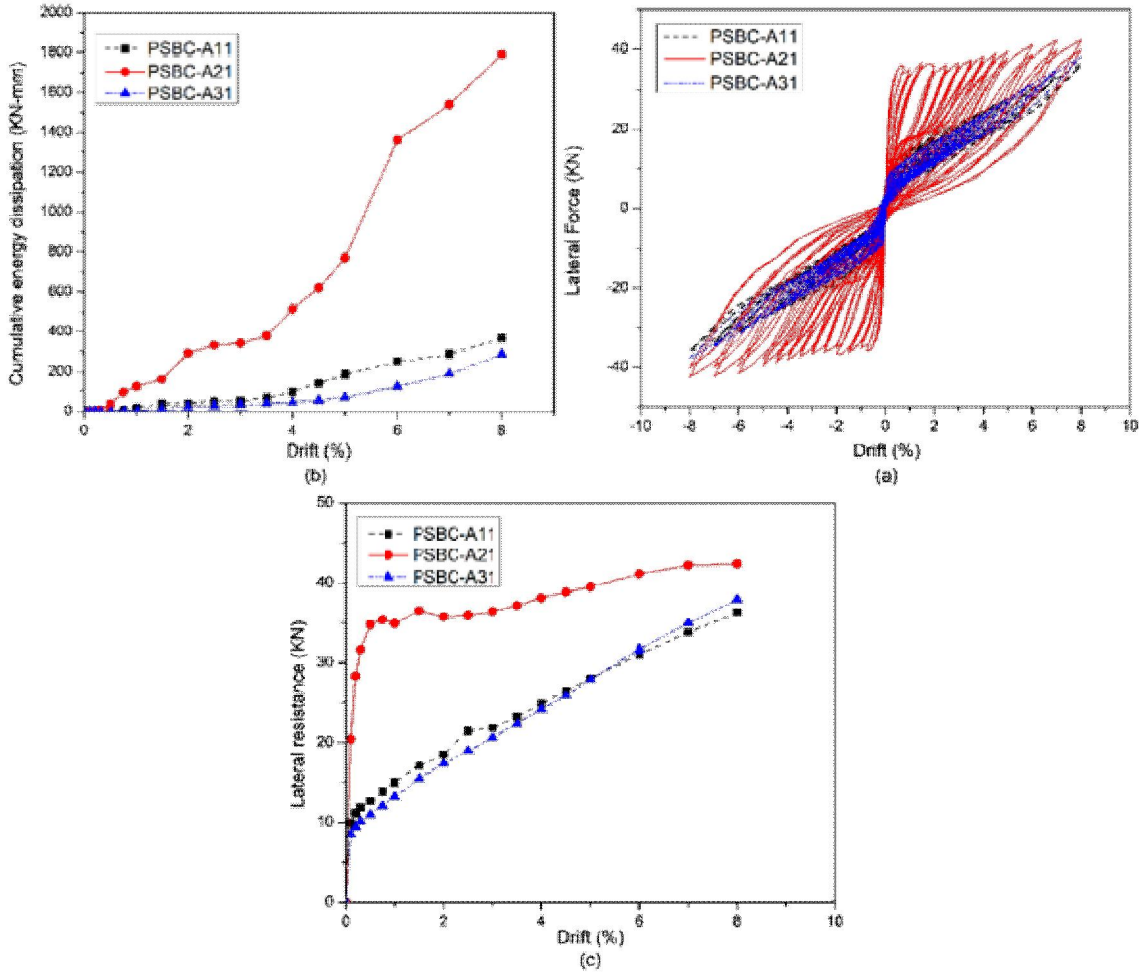

Fig. 12 Seismic characteristics of PSBCs with different orientations a) hysteric shapes b) energy dissipation c) lateral resistance

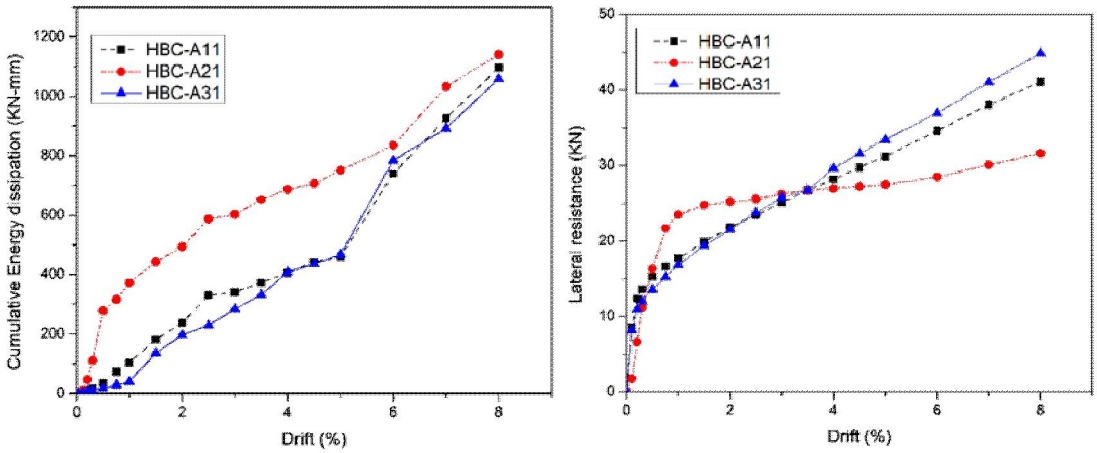

Fig. 13 Lateral resistance and cumulative energy dissipation capacities of HBCs

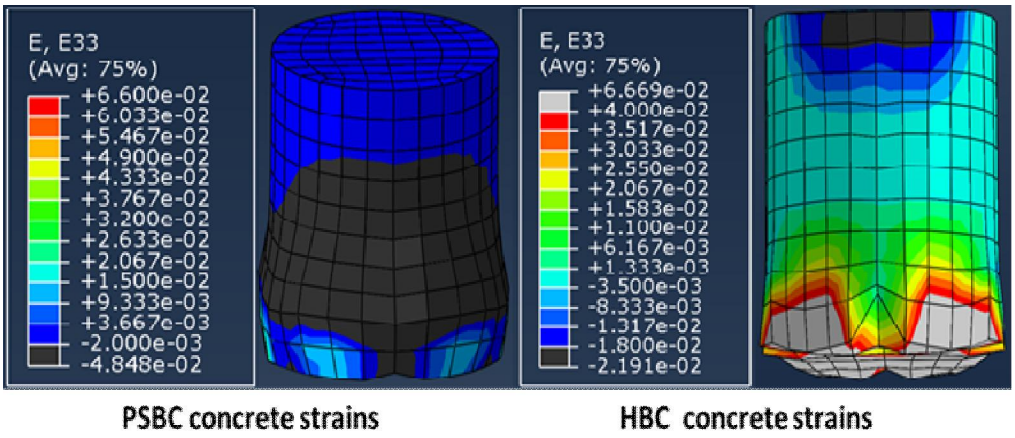

Fig. 14 Strains of PSBCs and HBCs specimens at ultimate drift

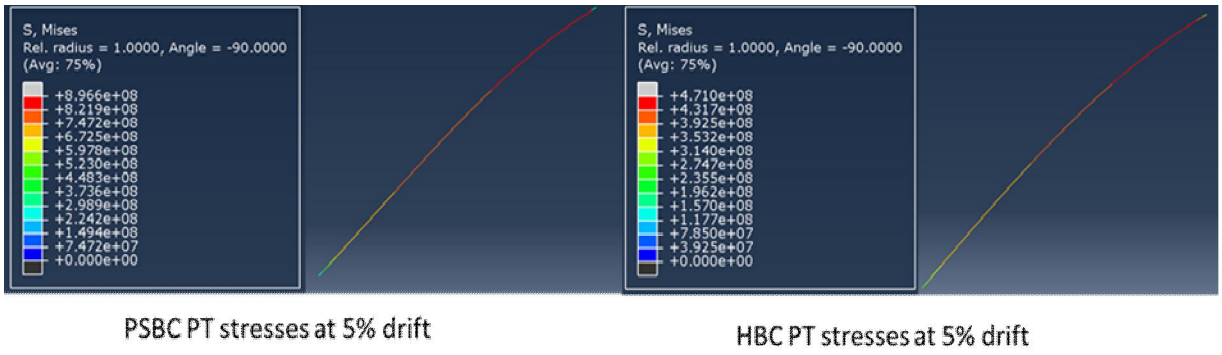

Fig. 15 Stresses of post-tensioned tendons oriented at the middle

HBC specimens with PT tendons oriented at the middle and edges showed similar characteristics to PSBCs in terms of the shape of the lateral resistance curves with a gradual increase in the lateral strength and energy dissipation. The HBCs were able to accumulate greater lateral strength and energy dissipation due to the cast-in-place bottom segment. At the initial stage, the HBC with tendons oriented at the middle showed improved lateral strength and energy dissipation than the specimens with tendons placed at the edges. For example, at 0.75%, the HBCs with tendons in the middle was able to generate 42% and 91% greater lateral strength and energy dissipation, as shown in **Fig. 13**. After 0.75%, the

softening of the lateral resistance curve occurs, which results in all specimens converging at a 3.5% drift. Later on, the influence of softening becomes more evident, hence resulting in much less lateral resistance at the ultimate stage of a pier for a specimen with PT tendons oriented at the geometric centroid. The energy dissipation capacities at the ultimate stage for HBCs with different orientations were similar, which validates the enhanced softening of the HBCs with PT tendons at the center, as shown in **Fig. 13**.

These findings are in contrast to the PSBCs with tendons in the middle. The reason for this can be attributed to the difference in the mechanism of these two structural systems. The non-linearity of the specimens in HBCs becomes more dominant than its PSBCs counterpart; this is due to sizeable damage of the bottom segment in terms of cosmetic damage of concrete, severe crushing, yielding of reinforcement and tensile cracking of concrete as shown in **Fig. 14**. Another critical factor is the ability of tendons to transfer the shear to the column. The HBCs with center tendons were able to transfer fewer stresses than the PSBCs, which resulted in lower lateral strength, as shown in **Fig. 15**. It may be concluded that the orientations play a significant role in the cyclic performance of segmental columns. The tendons oriented at the middle show greater lateral strength at the initial stages for both PSBCs and HBCs, but only for PSBCs at the ultimate stage. Due to the non-linearity of HBCs specimens, the softening effect becomes more dominant, hence resulting in lower strength at the ultimate stage. PSBCs with an axial load ratio of 0.1 and with tendons oriented at the middle showed excellent energy dissipation capacities. In contrast, the HBC energy dissipation at the ultimate stage was similar for all orientations, respectively.

4.6 Combined Influence of Axial Loads and Orientation of Post-Tensioned Tendons

The axial loads and orientations play a vital role in the cyclic performance of PSBCs and HBCs, as evident in the previous sections. The rise in the axial load leads to an increase in the lateral strength and the energy dissipation of specimens, as detailed in sections 4.1-4.4. The orientations of post-tensioned tendons highlight the differences in the seismic performance of PSBC's and HBCs, as shown in section 4.5. When the axial loads are kept constant (0.1), the post-tensioned tendons placed at the center show a better performance in PSBCs, whereas, for HBCs, the placement of post-tensioned tendons at the middle and only edges is a better option respectively. As the performance of HBCs with increasing axial load ratios for tendons oriented at the middle and edge is already discussed in section 4.3. Hence in this section, the combined influence of increased axial loads and two orientations (middle and edge, middle) are analyzed to further study their contribution to the seismic performance of PSBCs in order to select appropriate axial load ratios. The specimen details are described in **Table 6**.

The specimens with post-tensioned tendons positioned at the middle and edges show an increase in the lateral strength with an increment in the axial load ratio. No sign of softening or strength degradation is observed. On the other hand, the lateral strength curves of PSBCs having tendons at the center indicate a major difference with an increase in the axial load ratio. At the initial stages (up to 0.75% drift), there is a surge in the lateral resistance for all specimens, as evident in **Fig. 16**. After 0.75% drift, the softening action of lateral curves is dominant for the specimens with an axial load ratio of 0.1 and 0.15. The softening becomes more prominent with an extension in the axial load ratio as apparent by a gradual rise in the lateral strength beyond 0.75% drift for a specimen with an axial load ratio of 0.1. The peak strength is observed at the ultimate drift, whereas a slight deflection from peak value is observed at drifts over 0.75% for a specimen with a 0.15 axial load ratio. Increasing the axial loads beyond 0.15 resulted in significant strength degradation. The drop in the ultimate strength is observed as 25% of the peak strength. The peak strength is observed at 0.75% drift for a specimen with an axial load ratio of 0.2. The comparative analysis shows that increasing the axial loads beyond 0.1 for specimens with post-tensioned tendons placed at the geometric center results in lower strengths than their counterpart specimens.

Table 6 Specimen details for PSBCs with different axial loads and orientations of PT tendons

Specimen	Orientation of Post-tensioned tendons	Axial load ratio
PSBC-A11	Middle and edge	0.1
PSBC-A12	Middle and edge	0.15
PSBC-A13	Middle and edge	0.2
PSBC-A21	Middle	0.1
PSBC-A22	Middle	0.15
PSBC-A23	Middle	0.2

The energy dissipation curves are also shown in **Fig. 16**. The values of dissipated energy surge with a rise in the axial load ratios for all but PSBC-A23, whose value dropped by 21%. The substantial strength degradation and the greater number of drops observed along the cyclic loading drifts result in a drop in energy dissipation. The comparative analysis shows that piers with post-tensioned tendons in the middle can dissipate immense energy than specimens with tendons at the middle and edges. Overall, it can be concluded that the specimens with post-tensioned tendons oriented at the middle can perform better under cyclic loadings if the axial loads are maintained under 0.15. The energy dissipation capacities were still greater for the specimens having an axial load ratio of 0.2 and tendons positioned at the center than the ones with tendons at middle and edges. However, due to the substantial strength degradation and shreds of evidence of drops in the energy dissipation, along the cyclic loading drifts indicate the potential risks. Hence, an axial load ratio of 0.1-0.15 is suggested along with tendons placed at the geometric center for the columns constructed with similar construction shapes, reinforcement ratios, and aspect ratios, respectively.

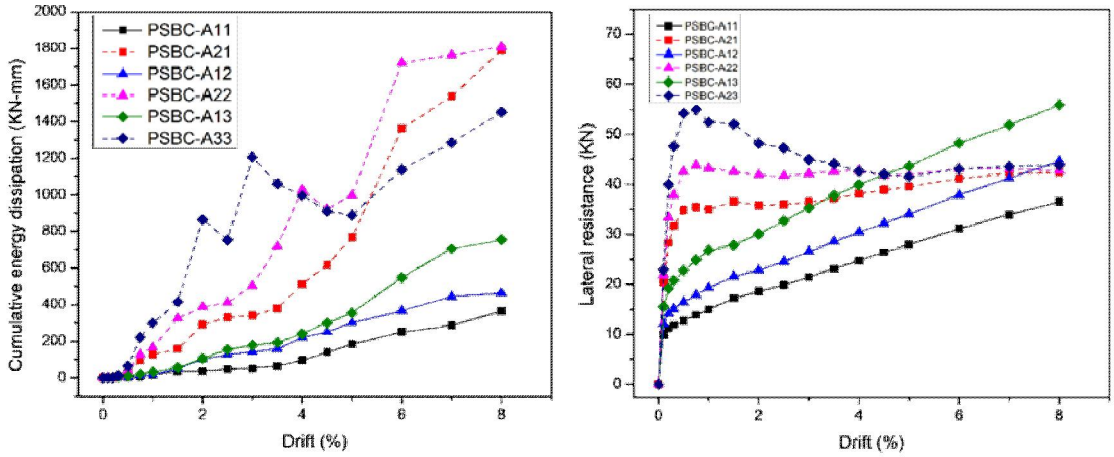

Fig. 16 Lateral resistance and cumulative energy dissipation curves of PSBS's with different axial loads and orientation of tendons

Table 7 Model details of HBCs with and without Hybrid bonded post-tensioned tendons.

Specimen	Bonding Condition	Post-tensioned tendon area	Bonded length in plastic hinge	Axial load ratio
HBC-PH1	Hybrid bonded	3D15.2mm	100mm	0.1
HBC-A1	Unbonded	3D15.2mm	-	0.1

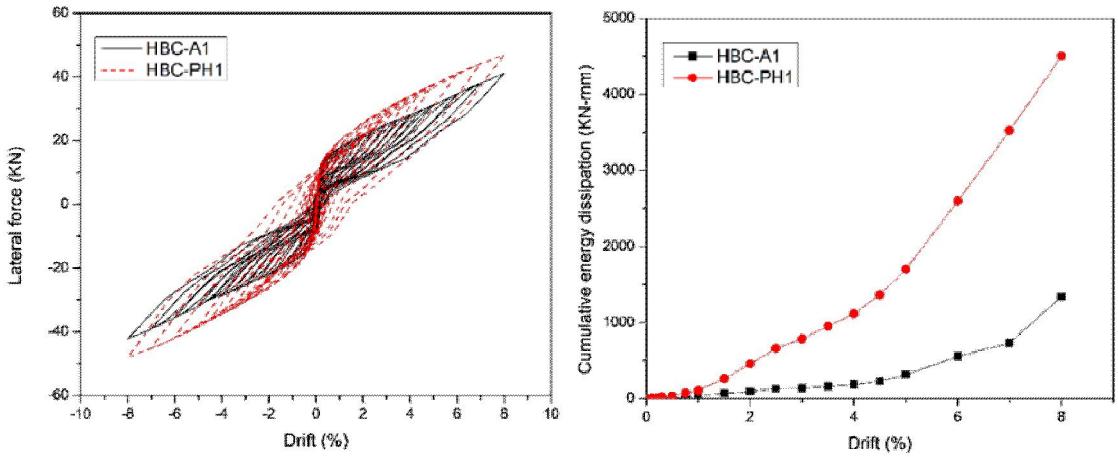

Fig. 17 Hysteric and energy dissipation curves of HBCs with unbonded and hybrid bonded post-tensioned tendons

4.1 Influence of Hybrid Bonded Post-Tensioned Tendons

The hybrid bonded tendons are an innovative and novel post-tensioned tendon system as compared

to the bonded and unboned ones. This section will study the influence of hybrid bonded tendons in the cyclic performance of hybrid bridge columns (HBCs). For that purpose, HBCs with and without the hybrid bonded tendons are selected for analysis. The model details are described in **Table 7**.

The damage was as-symmetric with a negative direction showing a slight increase in the ultimate lateral strength for both the specimens. Usage of hybrid bonded tendons in HBCs improved the lateral strength by 14%. There is a significant increase in HBC's energy dissipation with hybrid tendons; the maximum cumulative energy obtained is 4501 KN-mm, which is 70% greater than HBCs without hybrid tendons, respectively. The higher energy dissipation can be attributed to the higher lateral strength and residual deformations, which contribute towards gaining greater area enclosed by the cyclic curve at given drift, as shown in **Fig. 17**. Hybrid bonding leads to greater stresses induced in the column, which results in higher strength, but higher stress can cause greater strain concentrations and yield of reinforcements at the compression toe, as evident in **Fig. 18** with a bulging effect at the bottom joint of HBC. Considerable damage to the concrete surrounding the hybrid bonded tendons along with overall greater strain developed in the bottom segment results in HBCs gaining extensive damage and residual plastic deformation of a maximum 30mm (1.66% residual drift) in the negative direction.

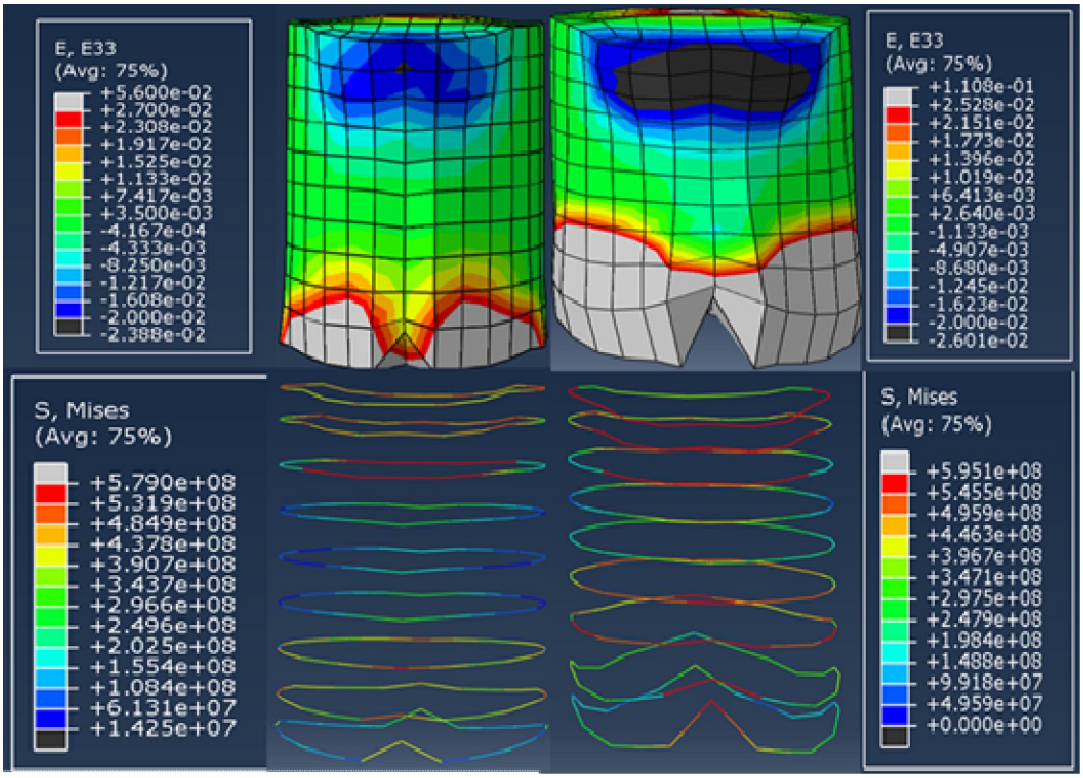

Fig. 18 Compressive strains and transverse stresses of HBCs bottom segment with and without hybrid bonded tendons

4.2 Comparitive Analysis of PSBCs and HBCs with Hybrid Bonded Tendons

The comparative analysis is done to evaluate the efficiency of hybrid bridge columns in different structural systems. The design parameters are shown in **Table 8**. The backbone curves of the specimens showed similar lateral strength. The energy dissipation increased with the increase in the bonded length of hybrid bonded tendons, as shown in **Fig. 19**. The major difference in the energy dissipation of PSBCs and HBCs with hybrid bonded tendons can be attributed to the combined effect of the development of plastic hinges at the bottom joint. Extensive damage to the concrete surrounding the hybrid bonded tendons, cover spalling and concrete crushing occurring at the upper joint of the bottom segment and yielding of transverse reinforcements. In contrast, the PSBCs will only have damage at the compression toe, due to rigid rotation and damage to the concrete surrounding the tendons. The hysteric curves in **Fig. 20** shows the crucial difference in the cyclic performance of the two structural systems afro-mentioned, whereas **Table 9** details the residual plastic deformation, respectively.

The major increase in the energy dissipation of HBCs with hybrid bonded tendons can be very beneficial in the usage of columns in different seismic regions. However, the residual plastic displacement can make these piers challenging to repair. In order to make this design more desirable for engineers, confinement of bottom segments should be improved. The excessive cosmetic and severe damage can be reduced by utilizing the carbon fiber reinforced polymers (CFRP) wraps [50-52]. Additionally, CFRP wraps have an advantage of improving the lateral strength along with maintaining the energy dissipation. In further studies, the CFRP wraps can be utilized in combination with the hybrid bonded tendons in the HBCs to make the design more efficient.

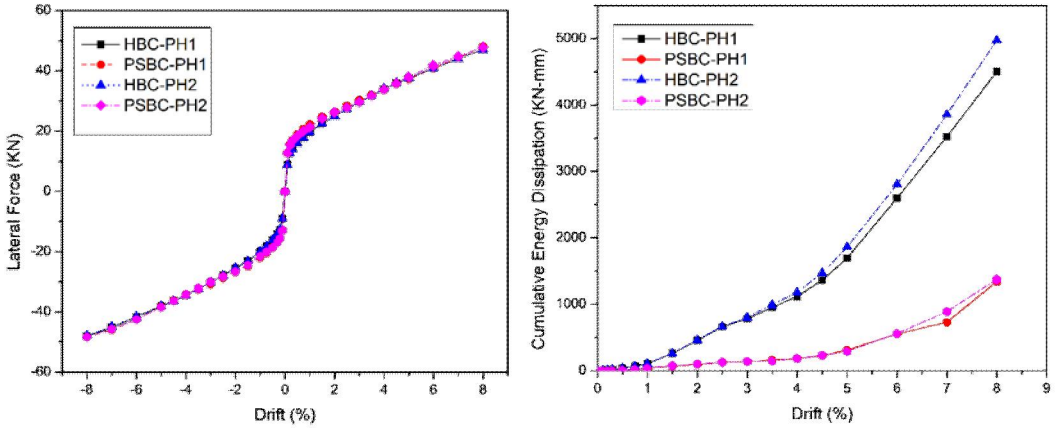

Fig. 19 Backbone and energy dissipation curves of PSBCs and HBCs with hybrid bonded tendons.

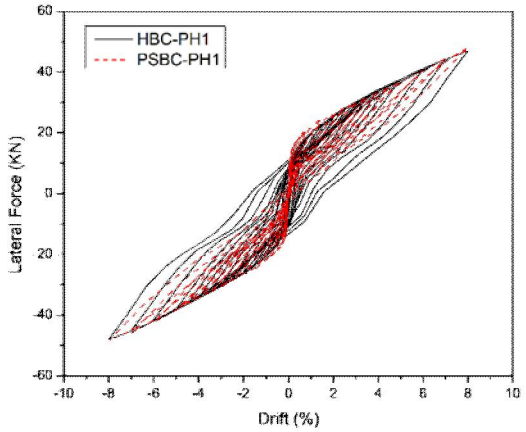

Fig. 20 Cyclic curves of HBCs and PSBCs with hybrid bonded tendons

Table 8 Design parameters of PSBCs and HBCs

Specimen	Bonding Condition	Post-tensioned tendon area	Bonded length in plastic hinge	Axial load ratio
PSBC-PH1	Hybrid bonded	3D15.2mm	100mm	0.1
PSBC-PH2	Hybrid bonded	3D15.2mm	200mm	0.1
HBC-PH1	Hybrid bonded	3D15.2mm	100mm	0.1
HBC-PH2	Hybrid bonded	3D15.2mm	200mm	0.1

Table 9 Residual displacement of PSBCs and HBCs

Specimen	Bonding Condition	Residual displacement (mm)
PSBC-PH1	Hybrid bonded	8.86, -5.96
PSBC-PH2	Hybrid bonded	9.2, -6.13
HBC-PH1	Hybrid bonded	27,-30
HBC-PH2	Hybrid bonded	33,-34

Conclusions

The significant findings of this paper are that the hybrid bridge columns fare better than the PSBCs under cyclic loadings with greater lateral strength and energy dissipation capacities. The increment in the axial loads increases the lateral resistance and energy dissipation capacity of both the PSBCs and HBCs. The residual plastic displacement remains within safety limits when the axial load ratios are carefully chosen. Hybrid bonded tendons performed impeccably in terms of lateral strength, energy dissipation for PSBCs. In contrast, for HBCs, the usage of hybrid bonded tendons significantly improved the energy dissipation capacity with much larger residual displacement. The residual displacement can be reduced by using greater confining reinforcements or by utilizing fiber-reinforced polymer (FRP) wraps, which will expectedly control excessive damage to the bottom segments of HBCs. When the axial loads are maintained below 1.5, the post-tensioned tendons positioned at the center of circular piers have superior cyclic performance than those positioned at the middle and edges or only at the edges of the PSBCs. For higher axial loads, the post-tensioned tendons should be located at the middle and edges. The post-tensioned tendons should be located at the middle and edges for HBCs to avoid excessive damage to the concrete and reinforcements, material non-linearity, softening, and strength degradation of lateral curves, respectively.

References

1. Federal Highway Administration. Seismic accelerated bridge construction workshop – Final Report, FHWA; 2007.
2. Wang Z, Qu H, Li T, Wei H, Wang H, Duan H, Jiang H (2018a) Quasi-static cyclic tests of precast bridge columns with different connection details for high seismic zones. Eng Struct 158:13–27.
3. Wang J, Wang Z, Tang Y, Liu T, Zhang J (2018b) Cyclic loading test of self-centering precast segmental unbonded posttensioned UHPFRC bridge columns. Bull Earthq Eng 16:5227–5255.
4. Shim CS, Chung CH, Kim HH. Experimental evaluation of seismic performance of precast segmental bridge piers with a circular solid section. Eng Struct 2008; 30 (12):3782–92.
5. Hällmark, R., White, H., & Collin, P. (2012). Prefabricated bridge construction across Europe and America. Practice Periodical on Structural Design and Construction, 17(3), 82-92.
6. Usami, T., & Ge, H. (2009). A performance-based seismic design methodology for steel bridge systems. Journal of Earthquake and Tsunami, 3(03), 175-193.
7. WANG, Z., GE, J., WEI, H., & LIU, F. (2009). Recent development in seismic research of segmental bridge columns [J]. Journal of Earthquake Engineering and Engineering Vibration, 4.
8. Dong, X., Li, H., & Liu, C. (2008). Precast segmental design and construction in China. Dept. Of Bridge Engineering, Tongji University, Shanghai, China.
9. Bu, Z. Y., Ding, Y., Chen, J., & Li, Y. S. (2012). Investigation of the seismic performance of precast segmental tall bridge columns. Structural Engineering and Mechanics, 43(3), 287-309.
10. Hewes JT, Priestley MJN. Seismic design and performance of precast concrete segmental bridge columns. Report No. SSRP-2001/25, University of California, San Diego, CA; 2002.
11. Dawood, H., ElGawady, M., & Hewes, J. (2011). Behavior of segmental precast posttensioned bridge piers under lateral loads. Journal of Bridge Engineering, 17(5), 735-746.
12. Li, C., Hao, H., & Bi, K. (2017). Numerical study on the seismic performance of precast segmental concrete columns under cyclic loading. Engineering Structures, 148, 373-386.
13. Wang, Z., Wang, J., Zhu, J., Zhao, G., & Zhang, J. (2019). Energy dissipation and self centering capacities of posttensioning precast segmental ultra high performance concrete bridge columns. Structural Concrete.
14. Ou, Y. C., Wang, P. H., Tsai, M. S., Chang, K. C., & Lee, G. C. (2009). Large scale experimental study of precast segmental unbonded posttensioned concrete bridge columns for seismic regions. Journal of Structural Engineering, 136(3), 255-264.
15. ElGawady MA, Sha'lan A. Seismic behavior of self-centering precast segmental bridge bents. J Bridge Eng 2011; 16 (3):328–39.
16. Roh H, Reinhorn AM, Lee JS. Modeling and cyclic behavior of segmental bridge column connected with shape memory alloy bars. Earthq Eng Eng Vibr 2012; 11(3):375–89.
17. Roh, H., & Reinhorn, A. M. (2010). Hysteretic behavior of precast segmental bridge piers with super elastic shape memory alloy bars. Engineering Structures, 32(10), 3394-3403.
18. Roh, H., Reinhorn, A. M., & Lee, J. S. (2012). Modeling and cyclic behavior of segmental bridge column connected with shape memory alloy bars. Earthquake Engineering and Engineering Vibration, 11(3), 375-389.
19. Mao, J., Jia, D., Yang, Z., & Xiang, N. (2019). Seismic Performance of Concrete Bridge Piers

Reinforced with Hybrid Shape Memory Alloy (SMA) and Steel Bars. Journal of Earthquake and Tsunami, 2050001.
20. Jia, J., Zhang, K., Saiidi, M. S., Guo, Y., Wu, S., Bi, K., & Du, X. (2020). Seismic evaluation of precast bridge columns with built in elastomeric pads. Soil Dynamics and Earthquake Engineering, 128, 105868.
21. ElGawady, M. A., & Sha'lan, A. (2010). Seismic behavior of self centering precast segmental bridge bents. Journal of Bridge Engineering, 16(3), 328-339.
22. Mohebbi, A., Saiidi, M. S., & Itani, A. M. (2018). Shake table studies and analysis of a precast two column bent with advanced materials and pocket connections. Journal of Bridge Engineering, 23(7), 04018046.
23. Trono, W., Jen, G., Panagiotou, M., Schoettler, M., & Ostertag, C. P. (2015). Seismic response of a damage-resistant recentering posttensioned-HYFRC bridge column. Journal of Bridge Engineering, 20(7), 04014096.
24. Ichikawa, S., Matsuzaki, H., Moustafa, A., ElGawady, M. A., & Kawashima, K. (2016). Seismic-resistant bridge columns with ultrahigh-performance concrete segments. Journal of Bridge Engineering, 21(9), 04016049.
25. Ou, Y. C., Oktavianus, Y., & Tsai, M. S. (2013). An emulative precast segmental concrete bridge column for seismic regions. Earthquake Spectra, 29(4), 1441-1457.
26. Kim DH, Moon DY, Kim MK, Zi G, Roh H (2015) Experimental test and seismic performance of partial precast concrete segmental bridge column with cast-in-place base. Eng Struct 100:178–188.
27. Zhang, Y., Fan, W., Zhai, Y., & Yuan, W. (2019). Experimental and Numerical Investigations on Seismic Behavior of Prefabricated Bridge Columns with UHPFRC Bottom Segments. Journal of Bridge Engineering, 24(8), 04019076.
28. Bu, Z. Y., Ou, Y. C., Song, J. W., Zhang, N. S., & Lee, G. C. (2015). Cyclic loading test of unbonded and bonded posttensioned precast segmental bridge columns with circular section. Journal of Bridge Engineering, 21(2), 04015043.
29. Chou, C. C., & Chen, Y. C. (2006). Cyclic tests of post tensioned precast CFT segmental bridge columns with unbonded strands. Earthquake Engineering & Structural Dynamics, 35(2), 159-175.
30. Nikbakht, E., Rashid, K., Hejazi, F., & Osman, S. A. (2014). A numerical study on seismic response of self centering precast segmental columns at different post tensioning forces. Latin American Journal of Solids and Structures, 11(5), 864-883.
31. Li, C., Hao, H., & Bi, K. (2017). Numerical study on the seismic performance of precast segmental concrete columns under cyclic loading. Engineering Structures, 148, 373-386.
32. Dawood, H., Elgawady, M., & Hewes, J. (2014). Factors affecting the seismic behavior of segmental precast bridge columns. Frontiers of Structural and Civil Engineering, 8(4), 388-398.
33. Wang, Z., Ge, J., & Wei, H. (2014). Seismic performance of precast hollow bridge piers with different construction details. Frontiers of Structural and Civil Engineering, 8(4), 399-413.
34. SIMULIA. 2012. ABAQUS 6.12 commercial computer software documentation. Providence, RI: SIMULIA.
35. Mander, J. B., Priestley, M. J., & Park, R. (1988). Theoretical stress strain model for confined concrete. Journal of Structural Engineering, 114(8), 1804-1826.
36. Lubliner, J., Oliver, J., Oller, S., & Oñate, E. (1989). A plastic damage model for concrete. International Journal of Solids and Structures, 25(3), 299-326.
37. Lee, J., & Fenves, G. L. (1998). Plastic damage model for cyclic loading of concrete structures. Journal of Engineering Mechanics, 124(8), 892-900.
38. Ou, Y. C., Tsai, M. S., Chang, K. C., & Lee, G. C. (2010). Cyclic behavior of precast segmental concrete bridge columns with high performance or conventional steel reinforcing bars as energy dissipation bars. Earthquake Engineering & Structural Dynamics, 39(11), 1181-1198.
39. Chen, W. R., Wang, T. C., & Yan, D. (2012). Concrete structure: Design principle of concrete structure.
40. Kulkarni, S. A., Li, B., & Yip, W. K. (2008). Finite element analysis of precast hybrid-steel concrete connections under cyclic loading. Journal of constructional steel research, 64(2), 190-201.
41. Zhang, Y. Y., & Zhai, Y. (2018). Improvements in seismic performance of prefabricated bridge piers. Journal of Highway and Transportation Research and Development (English Edition), 12(2), 43-50.
42. Chang, K. C., Tsai, M. S., Ou, Y. C., Wang, P. H., & Lee, G. C. (2012). Research and application of precast segmental concrete bridge columns in regions of high seismicity.
43. Wang, Z., Wang, J., Zhao, G., & Zhang, J. (2020). Modeling seismic behavior of precast segmental UHPC bridge columns in a simplified

method. Bulletin of Earthquake Engineering, 1-33.
44. Sideris, P., Aref, A. J., & Filiatrault, A. (2014). Large-scale seismic testing of a hybrid sliding-rocking posttensioned segmental bridge system. Journal of Structural Engineering, 140(6), 04014025.
45. Ichikawa, S., Matsuzaki, H., Moustafa, A., ElGawady, M. A., & Kawashima, K. (2016). Seismic-resistant bridge columns with ultrahigh-performance concrete segments. Journal of Bridge Engineering, 21(9), 04016049.
46. Hassanli, R., Youssf, O., Mills, J., & Fakharifar, M. (2017). Analytical Study of Force–Displacement Behavior and Ductility of Self-centering Segmental Concrete Columns. International Journal of Concrete Structures and Materials, 11(3), 489-511.
47. Nikbakht, E., & Rashid, K. (2018). Investigation on seismic performance and functionality of self-centering post-tensioned segmental columns. Structure and Infrastructure Engineering, 14(6), 730-742.
48. Bu, Z., Guo, J., Zheng, R., Song, J., & Lee, G. C. (2016). Cyclic performance and simplified pushover analyses of precast segmental concrete bridge columns with circular section. Earthquake Engineering and Engineering Vibration, 15(2), 297-312.
49. Yang, Y., Sneed, L. H., Morgan, A., Saiidi, M. S., & Belarbi, A. (2015). Repair of RC bridge columns with interlocking spirals and fractured longitudinal bars–An experimental study. Construction and Building Materials, 78, 405-420.
50. Miralami, M., Esfahani, M. R., & Tavakkolizadeh, M. (2019). Strengthening of circular RC column-foundation connections with GFRP/SMA bars and CFRP wraps. Composites Part B: Engineering, 172, 161-172.
51. Zhang, Y., Tabandeh, A., Ma, Y., & Gardoni, P. (2020). Seismic performance of precast segmental bridge columns repaired with CFRP wraps. Composite Structures, 112218.
52. Gu, D. S., Wu, Y. F., Wu, G., & Wu, Z. S. (2012). Plastic hinge analysis of FRP confined circular concrete columns. Construction and Building Materials, 27(1), 223-233.

6/20/2020